Fuel Processing Technology 123 (2014) 47–56

Contents lists available at ScienceDirect

Fuel Processing Technology

journal homepage: www.elsevier.com/locate/fuproc

Oxidation reactivity of chars generated from the acid-catalyzed pyrolysis of corncobs

Carmen Branca [a,*], Colomba Di Blasi [b]

[a] Istituto di Ricerche sulla Combustione, C.N.R., P.le V. Tecchio, 80125 Napoli, Italy
[b] Dipartimento di Ingegneria Chimica, dei Materiali e della Produzione Industriale, Università degli Studi di Napoli "Federico II", P.le V. Tecchio, 80125 Napoli, Italy

ARTICLE INFO

Article history:
Received 31 July 2012
Received in revised form 16 May 2013
Accepted 7 January 2014
Available online 22 February 2014

Keywords:
Biomass
Catalytic pyrolysis
Char
Oxidation
Kinetics

ABSTRACT

Thermogravimetric measurements are made in air, at three heating rates between 5 and 10 K/min, of chars produced from the pyrolysis of corncobs catalyzed by sulfuric acid, ferric sulfate and zinc chloride and, for comparison, of washed corncobs. The catalyst concentrations are those which maximize the furfural production and give rise to char yields between 27 and 32% (versus 22% in the absence of catalysts). The structural morphology and the reactivity, especially at high conversion, are largely affected by catalysts. Thus the kinetic evaluation also reveals that, although a two-step reaction mechanism is applicable in all cases, the estimated parameters are highly dependent on the catalytic treatment undergone by corncobs during the pyrolysis stage.

© 2014 Elsevier B.V. All rights reserved.

1. Introduction

The combined production of biofuels and bioproducts from biomass pyrolysis can increase significantly the process economics. However, for the majority of the compounds, the quantities are generally too small for practical applications. To obtain high yields of specific compounds, various factors need to be considered such as chemical composition of the substrate, addition of inorganic catalysts, catalyst profile and conditions of pretreatment and conversion. Thus, in the view of maximizing specific compounds, as a first step the "optimal" feedstock should be selected and adequate catalysts should be considered which are known to modify the relative yields and composition of the lumped classes of pyrolysis products. Extensive experimental investigations have been carried out in the last few years to determine the biomass and catalysts that can maximize the production via biomass pyrolysis of furfural [1–6]. This is one of the starting materials for nylon and is also used in refining motor oils, as a precursor of certain plastics and a cleaning agent in liquid fuels.

It has been found [7] that higher quantities of furfural are obtained from feedstocks with high contents of cellulose/pentoses, in particular corncobs. Moreover, the formation of this compound is enhanced by pre-impregnated acidic catalysts. The yields depend on the nature of the catalyst and the catalyst concentration. Maximum actual yields, for moderate heating temperatures which limit the activity of secondary decomposition reactions, are around 5–6% for the treatments with sulfuric acid (H_2SO_4,), ferric sulfate ($Fe_2(SO_4)_3$) and zinc chloride ($ZnCl_2$), with potential further increase, following secondary degradation of the main anhydrosugars, up to 6.5% ($ZnCl_2$), 8.5% (H_2SO_4) or 10% ($Fe_2(SO_4)_3$) [6].

Together with furfural, the acidic pyrolysis of corncobs also gives significant amounts of other products such as acetic acid and mainly char which is, from the quantitative point of view, the most abundant product. For the conditions that maximize the production of furfural, char yields are around 27–32% (versus 22% of uncatalyzed pyrolysis) (yields of organics, gas and water are around 20–23%, 10–11% and 27–29% versus 38, 13 and 20% of uncatalyzed pyrolysis, respectively) [6]. There are numberless applications of char which include [8,9] domestic cooking, refining of metals (copper, bronze, steel, silicon, nickel, aluminum, and electro-manganese), production of chemicals (carbon disulfide, calcium carbide, silicon carbide, sodium cyanide, soil conditioners and various pharmaceuticals), manufacture of fireworks and production of activated carbon. However, chars produced from the acid-catalyzed pyrolysis are expected to present properties and reactivities different from those of un-catalyzed pyrolysis, owing in the first place to the presence of the additives and/or products generated from their physico-chemical transformations associated with the thermal treatment. Moreover, the modifications induced by the catalysts in the decomposition reaction paths not only alter the yield of char but also its intrinsic properties. The oxidation characteristics of biomass chars have been given considerable attention [10–21], but similar information on the chars produced from acid-catalyzed pyrolysis is scarce. It is known that some acidic catalysts, such as ammonium salts [22,23] and boric acid [24], lower the oxidation rate, whereas iron sulfates [25] act as enhancers for the oxidation rate at low temperatures.

In this study, thermogravimetric curves are measured in air, for different heating rates, of chars obtained from the pyrolysis of corncobs

---

* Corresponding author. Tel.: +39 081 7682232; fax: +39 081 5936936.
E-mail address: branca@irc.cnr.it (C. Branca).

0378-3820/$ – see front matter © 2014 Elsevier B.V. All rights reserved.
http://dx.doi.org/10.1016/j.fuproc.2014.01.044

Table 1
Char yield from the pyrolysis of washed and impregnated (H_2SO_4, $ZnCl_2$, $Fe_2(SO_4)_3$) corncobs, catalyst content in corncobs, final solid mass fraction, Y_f, and elemental composition of the various samples (data for washed fir wood are also included for comparison).

	Washed	H_2SO_4	$ZnCl_2$	$Fe_2(SO_4)_3$	Washed fir wood
Char yield [wt.%]	22	28	32	29	22
Catalyst content in corncobs [wt.%]	0	2.1	4.8	3.7	0
Y_F	0.046	0.020	0.140	0.125	0.0
C [%]	81.2	82.5	75.2	77.4	80.3
H [%]	3.4	3.4	3.0	3.3	3.5
N [%]	0.2	0.2	0.2	0.3	<0.1

catalyzed by H_2SO_4, $Fe_2(SO_4)_3$ and $ZnCl_2$ and, for comparison purposes, of chars from un-catalyzed pyrolysis. In addition to the evaluation of the oxidation reactivity, the curves are used for a simultaneous kinetic analysis, leading to the formulation of a semi-global reaction mechanism and the related kinetic parameters. Also the physical structure of chars is studied by means of Scanning Electron Microscope (SEM) and X-ray diffraction (XRD) methods.

2. Materials and methods

2.1. Materials

Chars were produced from the packed-bed pyrolysis of corncobs, instantaneously exposed to a heating temperature of 800 K, as described in [6,7]. In brief, pyrolysis experiments were made with particles approximately 5 mm thick which gave rise to a packed-bed density of 0.15 g/cm^3. Before impregnation, particles were washed in hot (333 K) twice-distilled water (1 L for 100 g) for 2 h and with stirring to remove, in part, alkali compounds, thus reducing their catalytic action on the conversion process. Char obtained from the washed corncobs is indicated in the following as “washed char”. Impregnated corncob samples were obtained by soaking the sample in aqueous solutions (100 g for 0.5 L) for 3 h with stirring. The selected concentrations of the acidic catalysts, for the analysis of the char reactivity, are those which produce maximum yields of furfural and correspond to 2% (H_2SO_4), 3.7% ($Fe_2(SO_4)_3$) and 4.8% ($ZnCl_2$) on a dry feedstock basis. Chars obtained from these samples are indicated in the following as H_2SO_4, $Fe_2(SO_4)_3$ and $ZnCl_2$ treated samples.

The char is milled and then subjected to oxidation in air using the same thermogravimetric system already used in previous studies about solid fuel conversion (see, for instance, Refs. [15,20,23]). More precisely, the samples are milled to powder (particle sizes below 100 μm) and pre-dried for 10 h at 373 K. The conditions of the tests (4 mg of char distributed over a surface 25 mm × 5 mm) guarantee negligible heat and mass transfer limitations, as observed by varying the initial sample mass. Moreover, this system allows for a continuous monitoring and control of the actual sample temperature. Each curve is made in triplicate showing a good repeatability. Measurements are made at three heating rates, 5, 7.5 and 10 K/min, up to a final temperature of 873 K for the samples obtained from the acid-catalyzed pyrolysis. For comparison purposes, the same measurements are also carried out for the char obtained from the pyrolysis of washed corncobs.

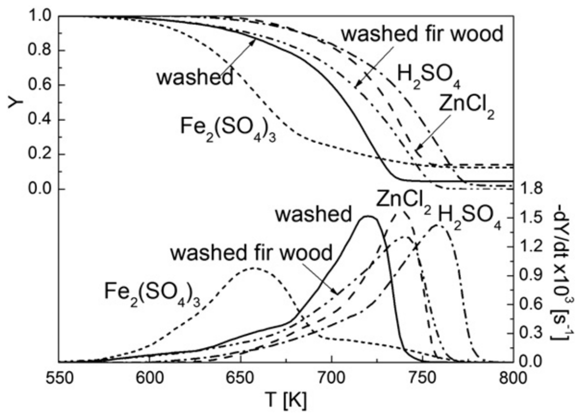

Fig. 1. Mass fraction and time derivative of the mass fraction versus temperature for chars produced from washed fir wood and corncobs and from impregnated (H_2SO_4, $ZnCl_2$, $Fe_2(SO_4)_3$) corncobs (heating rate 5 K/min).

2.2. Kinetic modeling

Conversion of lignocellulosic chars in oxidizing environments is usually described by means of two reactions, associated with devolatilization and combustion [26] (generally devolatilization refers to solid degradation in oxidative environments while pyrolysis refers to solid degradation in inert environment). The former process considers the release of relatively small amounts of volatile matter (about 15–20%), mainly depending on the nature of the precursor (including the presence of catalysts) and the formation conditions (for instance, temperature and heating rate). It is clearly evident for chars produced from both thermogravimetric experiments (in this case it is preceded by the devolatilization of the biomass sample [27–32]) and separated pyrolysis experiments [15,19,20,23,24]. Moreover the inclusion of the devolatilization reaction plays a crucial role for a correct evaluation of the activation energy of the oxidation reaction as typical values vary from about 100 kJ/mol (one-step global mechanism) to about 180 kJ/mol (two-step mechanisms) [26]. Thus, based on previous findings and the analysis of the measurements made in this study, char conversion in air is described by two reactions, corresponding to devolatilization and combustion of char:

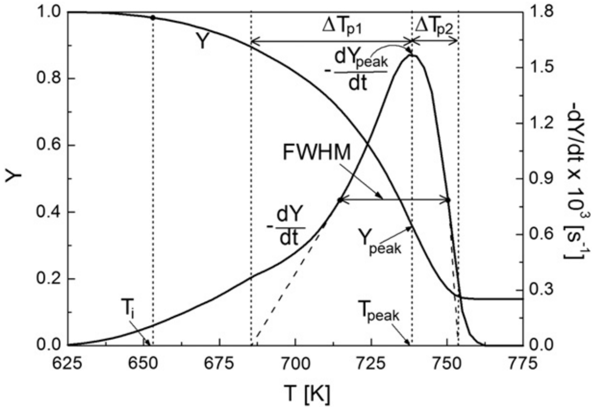

Fig. 2. Integral and differential thermogravimetric curves with the definition of characteristic parameters: initial degradation temperature, T_i, corresponding to 2% release of volatile products, peak rate, $-(dY/dt)_{peak}$, and corresponding mass fraction, Y_{peak}, and temperature, T_{peak}, mass fraction of the final solid residue, Y_f, full width of the rate curve at half maximum, FWHM, and temperature ranges determined by the position of the peak and the intercepts (on the temperature axis) obtained by extrapolating the tangents at the points of the FWHM, ΔT_{p1} and ΔT_{p2}.

Table 2
Characteristic parameters of the thermogravimetric curves for the char samples obtained from washed and impregnated (H_2SO_4, $ZnCl_2$, $Fe_2(SO_4)_3$) corncobs and washed fir wood for a heating rate of 5 K/min.

Characteristic parameters	Washed	H_2SO_4	$ZnCl_2$	$Fe_2(SO_4)_3$	Washed fir wood
T_i [K]	603	641	653	588	568
T_{peak} [K]	720	756	738	661	739
Y_{peak}	0.29	0.29	0.37	0.56	0.22
$-(dY/dt)_{peak} \times 10^3$ (s^{-1})	1.54	1.43	1.57	0.97	1.31
Y_f	0.046	0.02	0.076	0.125	0.0
FWHM [K]	42	44	36	58	55
ΔT_{p1} [K]	55	60	50	70	78
ΔT_{p2} [K]	17	20	15	42	19

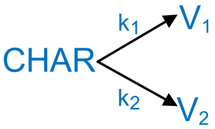

It is worth noticing that parallel reactions permit the description of both sequential and overlapping processes by an appropriate set of parameter values. The reaction rates present the usual Arrhenius dependence on temperature (A_i are the pre-exponential factors and E_i the activation energies). The combustion reaction foresees a power law dependence on the solid mass fraction (exponent n_2) which can effectively take into account the evolution of the pore surface area during this process [26]. Following previous treatments [26], given that the oxygen concentration is constant in the experiments, its effects are simply incorporated in the pre-exponential factor. The devolatilization reaction for chars produced from untreated biomass shows a linear dependence on the mass fraction [26]. However, in this study, given that catalysts may promote oxidation even at low temperature, for the sake of generality, a power law dependence on the solid mass fraction is also included for this reaction (exponent n_1). The estimated n_1 values will testify whether oxidation in the first stage is important or not. Since the sample temperature is a known function of time, the mathematical model consists of two ordinary differential equations for the mass fractions, Yi, of the two lumped groups of volatile species whose initial values (stoichiometric coefficients) are indicated with ν_i (in other words, these represent the final mass fractions of volatile species produced from each reaction). The kinetic parameters are estimated through the numerical solution of the mass conservation equations and the application of a direct method for the minimization of the objective function, which considers both integral (TG) and differential (DTG) data, following the method already described [33,34]. The simultaneous use of experimental data measured for several heating rates avoids possible compensation effects in the kinetic parameters [35,36]. Deviations between measurements and model predictions, dev_{TG} and dev_{DTG}, are defined as in [33].

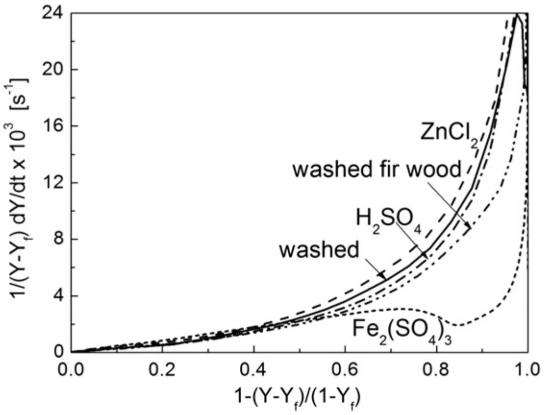

Fig. 3. Reactivity versus conversion for chars produced from washed fir wood and corncobs and from impregnated (H_2SO_4, $ZnCl_2$, $Fe_2(SO_4)_3$) corncobs (heating rate 5 K/min).

3. Results

Char examined are those produced from the packed-bed pyrolysis, at a heating temperature of 800 K, of washed corncobs and corncobs impregnated with H_2SO_4, $Fe_2(SO_4)_3$ and $ZnCl_2$ with concentrations giving maximum yields of furfural [6]. Thermogravimetric curves, measured at variable heating rates, of the various char samples in air are analyzed in terms of characteristic parameters and reactivity. The morphological structure of the char samples as determined by SEM and XRD is also discussed. Then the results of the kinetic modeling are presented including parameter estimation.

Table 1 summarizes the chief characteristics of the pyrolysis process (char yields and catalyst concentration in the corncob samples) and the char samples (contents of C, H and N for the char samples with a moisture content around 5%, and final solid residues, Y_f, obtained in air from ambient conditions up to 873 K for the range of heating rates investigated). It can be observed that the C content (about 81–82%) is about the same for the washed and the H_2SO_4 treated samples. For these samples the final solid residue is rather small, especially for the latter. Indeed, it is plausible that the aqueous impregnation of the corncob particles with a highly acidic solution also contributes in ash leaching. On the other hand, at the pyrolysis conditions, the acid decomposes to SO_3 and H_2O, without any solid-phase product [6]. Therefore, from the chemical point of view the two char samples exhibit similar properties, although the treatment with the acid increases the yield of this product and modifies the porous structure. The solid residue, detected at 873 K in air, can be essentially ascribed to the indigenous inorganic matter originally present in the biomass. The C content is significantly lower for the other two char samples corresponding to about 75 and 77% for the treatments with $ZnCl_2$ and $Fe_2(SO_4)_3$, respectively. It is plausible that that a significant part of the additives remains in the solid-phase, resulting in a lowered C content. Therefore, the added catalysts modify the yield and properties of chars produced during the pyrolysis stage and may also directly affect the occurrence of the oxidation reactions.

3.1. Reactivity and morphological structure

The integral (TG) and differential (DTG) weight loss curves obtained for the various samples at a heating rate of 5 K/min are shown in Fig. 1. For comparison purposes the data obtained under the same conditions for washed fir wood [23] are also reported. The characteristic parameters are defined through Fig. 2 and listed in Table 2. They include the initial degradation temperature, T_i, corresponding to 2% release of volatile products, the peak rate, $-(dY/dt)_{peak}$, and the corresponding mass fraction, Y_{peak}, and temperature, T_{peak}, the mass fraction of the final solid residue, Y_f, the full width of the rate curve at half maximum, FWHM,

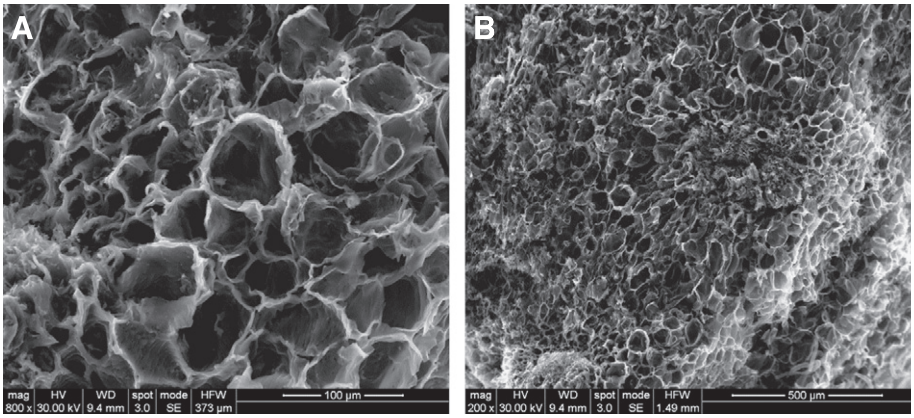
A
B
mag HV WD spot mode HFW
800 x 30.00 kV 9.4 mm 3.0 SE 373 μm
100 μm
mag HV WD spot mode HFW
200 x 30.00 kV 9.4 mm 3.0 SE 1.49 mm
500 μm

Fig. 4. A–B — SEM pictures of the cross (perpendicular to the cob fibers) surface of washed corncob char.

[37], and the temperature ranges determined by the position of the peak and the intercepts (on the temperature axis) obtained by extrapolating the tangents at the points of the FWHM, ΔT_{p1} and ΔT_{p2}. It can be observed that, in the absence of added catalysts, the rate of weight loss is constituted by two main zones as already found for wood chars: at low temperatures a wide zone of a relatively low rate (usually devolatilization) is followed by a peak (usually oxidation) which then rapidly goes to zero. The comparison with results obtained with washed fir wood shows that the corncob char is oxidized at lower temperature (T_{peak} value of 720 K versus 739 K), most likely as a result of the higher contents of indigenous alkalis that are not completely removed by mild water washing. The different chemical structure of the hemicellulose and lignin components may also be another cause for this difference [32]. The weight loss curves obtained with the H_2SO_4 and $ZnCl_2$ treatments are qualitatively similar, in relation to the devolatilization and oxidation zones, to that obtained for the washed corncob char. However, they are displaced at higher temperatures, especially in the case of the H_2SO_4 treatment, in relation to both the beginning of the process (T_i values of 653 and 641 for $ZnCl_2$ and H_2SO_4 versus 603 K) and the attainment of the peak rate (corresponding T_{peak} values of 738 and 756 versus 720 K). The peak rates are comparables for these three samples but, as a consequence of the significantly larger solid residue, the mass fractions in correspondence of the peak, Y_{peak}, is higher for the $ZnCl_2$ treatment. The qualitative trend of the sample treated with $Fe_2(SO_4)_3$ is different. It shows a zone of relatively high rates of weight loss at low temperatures followed by a gradual decrease, in accordance with the results reported in [25]. Indeed, the beginning of the process is anticipated at 588 K and the peak rate is attained at a temperature of 661 K. The second zone of slow weight loss is quite wide but the process terminates at about the same temperature as in the absence of added catalysts. On the average, the weight loss rates are lower compared with those shown by the other chars.

The parameters FWHM, ΔT_{p1} and ΔT_{p2} provide a quantitative evaluation of the shape of the rate curves and thus of the actual oxidation rates, independently from the temperatures at which the peak rates are attained. Washed corncob char presents lower values of all these three parameters, compared with wood, testifying the occurrence of the main oxidation stage with faster rates. More precisely, a large part of the conversion occurs over a narrower temperature range and the initial rise and final decay of the oxidation rate are sharper. The shape parameters are slightly higher for the H_2SO_4 treated char with respect to the washed sample, evidencing that, with reference to their respective peak temperatures, the oxidation process is slower. On the other hand, the $ZnCl_2$ treated sample presents a lower FWHP value, also associated with smaller values for ΔT_{p1} and ΔT_{p2}, indicating that, in the neighborhood of its peak temperature, the oxidation rate is the highest compared with the other samples. For the $Fe_2(SO_4)_3$ treated sample the parameters characterizing the shape of the rate curve around the peak are much higher, testifying that the reaction process is very slow. Finally, the parameters describing the thermogravimetric curves remain qualitatively the same as the heating rate is increased but the characteristic temperatures are displaced towards higher values.

A further comparison between the various samples can be made by means of the reactivity curves, $R = 1/(Y-Y_f)\ dY/dt$, versus conversion, 1-

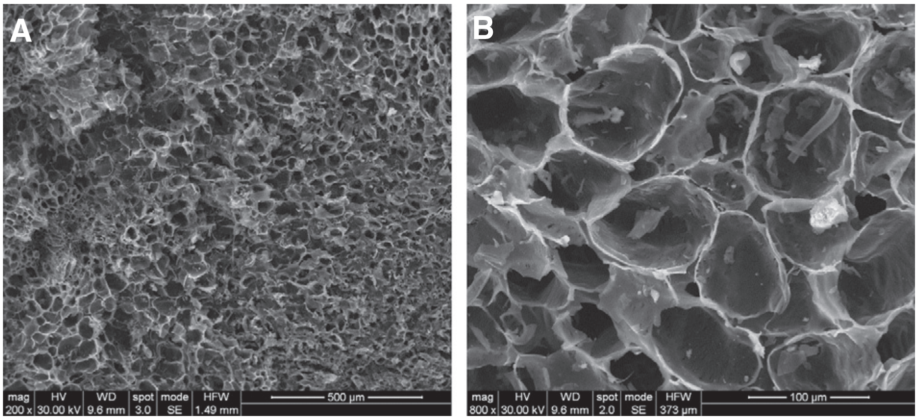
A
B
mag HV WD spot mode HFW
200 x 30.00 kV 9.6 mm 3.0 SE 1.49 mm
500 μm
mag HV WD spot mode HFW
800 x 30.00 kV 9.6 mm 2.0 SE 373 μm
100 μm

Fig. 5. A–B — SEM pictures of the cross (perpendicular to the cob fibers) surface of H_2SO_4-treated corncob char.

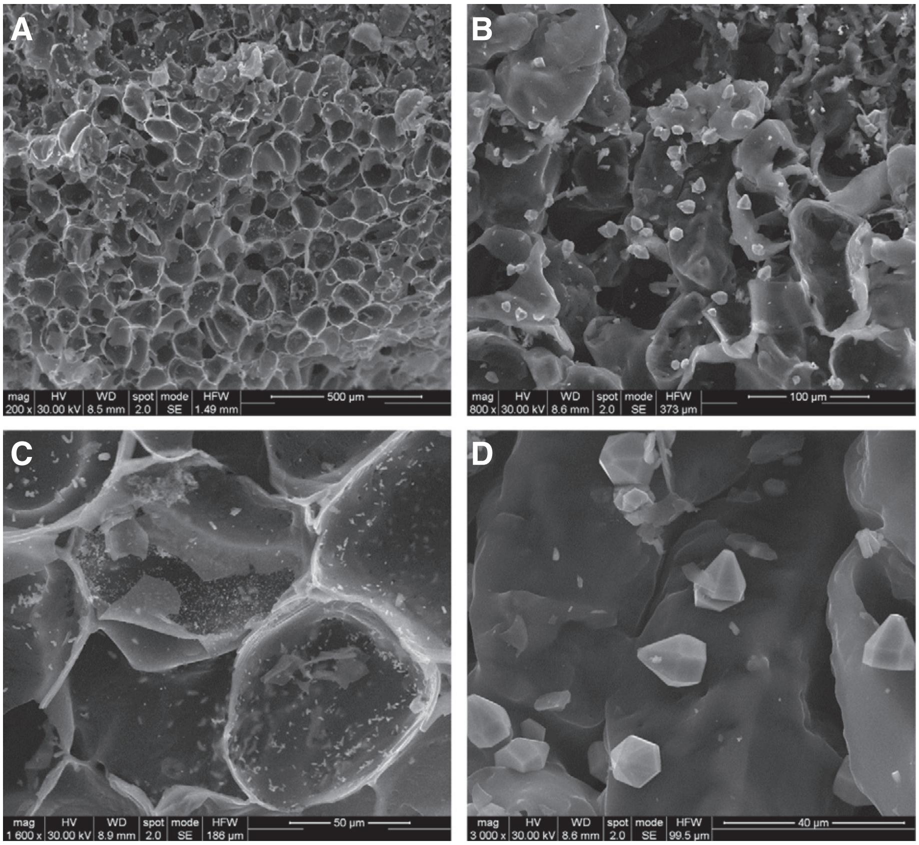
A
B
C
D
mag HV WD spot mode HFW
200 x 30.00 kV 8.5 mm 2.0 SE 1.49 mm
500 μm
800 x 30.00 kV 8.6 mm 2.0 SE 373 μm
100 μm
1 600 x 30.00 kV 8.9 mm 2.0 SE 186 μm
50 μm
3 000 x 30.00 kV 8.6 mm 2.0 SE 99.5 μm
40 μm

Fig. 6. A–D — SEM pictures of the cross (perpendicular to the cob fibers) surface of $ZnCl_2$-treated corncob char.

$(Y-Y_f)/(1-Y_f)$, reported in Fig. 3 (heating rate 5 K/min). As expected, in all cases, the reactivity increases with the conversion, due essentially to an increase in the surface area for the heterogeneous reaction [26]. For conversions below 50%, the differences between the various samples are small (possibly within the error bars of the experiments), despite the different thermal stability shown in Fig. 1. At high conversions (values above 50% for the $Fe_2(SO_4)_3$ treated sample and above 80% for the other two catalysts), the chars obtained from the acid-catalyzed pyrolysis present a lower reactivity. This is due to the very low rate of volatile release ($Fe_2(SO_4)_3$, with high values of the parameters FWHM and ΔT_{p1} and ΔT_{p2}) and/or to the less steep decay after the peak rate (H_2SO_4 and $ZnCl_2$ with high values of ΔT_{p2}). The same consideration applies for the fir wood with respect to the corncob char.

Figs. 4–7 report the SEM pictures of the char from washed corncobs and acid-treated corncobs with reference to the cross section, that is, that perpendicular to the fiber direction. In all cases, the typical porous structure is shown which, compared to wood [20], is less ordered. The char structure is not significantly different between the char produced from washed corncobs (Fig. 4A–B) and the H_2SO_4 treated corncobs (Fig. 5A–B), apart from thicker walls of the cellular structure in the latter case owing to the higher yield of the solid product. For both cases, the XRD analysis reports the presence of hydrated compounds containing Mg, Na, Al, P, N and S (sometimes as sulfates) originated by the indigenous inorganic matter, in accordance with the assumption that no significant solid phase residues are formed from the evolution of H_2SO_4 during pyrolysis. The reduced content of indigenous matter content, following acid leaching, can play an important role in the reduced reactivity of the chars obtained from the H_2SO_4 treatment.

During pyrolysis, $ZnCl_2$ undergoes melting (around 558 K) and starts to evaporate at temperatures above 773 K [38]. SEM pictures (Fig. 6A–D) show the presence of white crystals that, based on XRD analysis, appear to be ZnO that is most likely formed owing to the action of oxygenated tar vapors during the pyrolysis process. These solid compounds tend to cover part of the porous structure of the char substrate. The displacement of the oxidation process at higher temperatures, in the presence of $ZnCl_2$, is in agreement with the role played by this catalyst as inhibitor for the smoldering combustion of cotton cellulose [39]. Moreover, it is possible that the significant amount of residues generated from the catalysts also hinders the diffusion of oxygen towards the active sites of the char structure.

SEM pictures (Fig. 7A–F) show that the treatment with $Fe_2(SO_4)_3$ gives rise to a surface layer of brittle material that, in part, covers the char structure. It is reported [40] that, in oxidizing environments plausibly caused by the release of highly oxygenated tarry compounds, this catalyst does not decompose directly to Fe_2O_3 but to some intermediate oxo-sulfates, such as $Fe_{12}O_3(SO_4)_{15}$, (together with the release of SO_2). These salts are formed around 748 K whereas Fe_2O_3 appears at temperatures of 773–1033 K. On the other hand, the XRD analysis reveals the presence of Fe_2O_3 which gives rise to spherically-shaped crystals (Fig. 7F). It can be speculated that oxo-sulfates are present in a molten phase, justified by the presence of unexploded bubbles (Fig. 7D) and filaments (Fig. 7E), forming high surface area catalysts which then are highly active in promoting the oxidation of char at low temperature [39]. More precisely, iron sulfates have little effect on the chemisorption of oxygen but are able to enhance the rate of gasification [25,41,42]. The mechanism of catalysis of oxidation by metal salts is believed [39] to be due to the effects of dissociation of molecular oxygen and transfer of atomic oxygen in contact with the metal catalyst. Thus the catalytic action of iron compounds can explain the first zone of low-temperature oxidation shown by the curves reported in Fig. 1. Several explanations are possible for the second low-rate zone. There may be a rapid

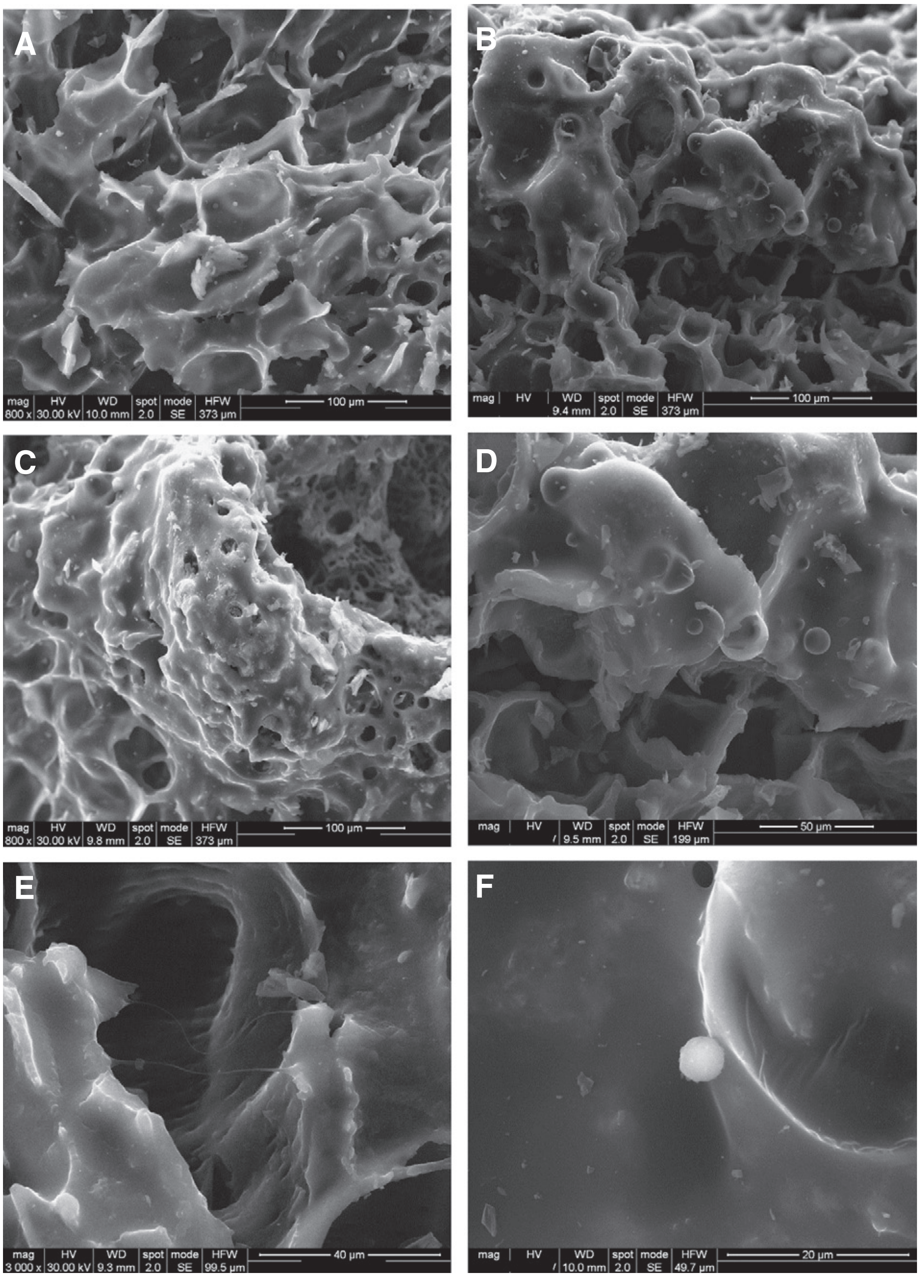

Fig. 7. A–F — SEM pictures of the cross (perpendicular to the cob fibers) surface of $Fe_2(SO_4)_3$-treated corncob char.

consumption of active sites [25], so that the second zone of the curve is related to the oxidation of the less accessible part of the char. Furthermore there can be a rapid consumption of the char in direct contact with the catalyst which, as shown by the SEM pictures, is not uniformly distributed. Once this char part is depleted, the remaining part undergoes oxidation with a rate comparable to that of chars obtained in the absence of catalyst. The thermal program during the thermogravimetric test, together with the presence of oxygen, may also cause changes (and possible partial deactivation) of the catalyst. Finally, the increasing proportion between the amount of iron compounds and char also make successively more difficult the diffusion of oxygen towards the reaction surface.

There is also another consideration that can be made in relation to the different reactivity of the chars produced from un-catalyzed pyrolysis and the acid-catalyzed pyrolysis. Cellulosic chars consist of aliphatic and aromatic groups [43]. The aliphatic groups are made of paraffinic, carbonyl and carboxyl functionalities. These, which are less stable than the aromatic groups, are preferentially decomposed, and condensation and cross-linking of the residue form a char composed predominantly of polycyclic aromatic structures carrying a high concentration of resonance stabilized free radicals. Thus the aliphatic groups are oxidized at temperatures lower than those needed for the oxidation of the more stable aromatic structures. Acidic additives enhance char formation by catalyzing the dehydration and decomposition reactions. Moreover, they also alter the composition of intermediate chars [43]. Contrary to un-catalyzed pyrolysis, where aromatic components are formed at high temperatures, in the presence of acidic substances, these already appear at the beginning of the decomposition process when the temperature is still low [44]. Therefore the more aromatic structure of chars produced from the low-temperature and acid-catalyzed pyrolysis may be another possible reason for the reduced reactivity.

Table 3
Estimated kinetic parameters and deviations between measurements and predictions for the char samples obtained from washed and impregnated (H_2SO_4, $ZnCl_2$, $Fe_2(SO_4)_3$) corncobs and washed fir wood (ν_{1a} and ν_{2a} indicate the average (constant) values of the stoichiometric coefficients).

Sample treatment	Washed			H_2SO_4			$ZnCl_2$			$Fe_2(SO_4)_3$			Washed fir wood		
Stage 1	$E_1 = 123.5$ [kJ/mol] $A_1 = 2.21 \times 10^7$ [s^{-1}] $n_1 = 1.00$			$E_1 = 131.7$ [kJ/mol] $A_1 = 2.66 \times 10^7$ [s^{-1}] $n_1 = 1.00$			$E_1 = 210.0$ [(kJ/mol] $A_1 = 5.68 \times 10^{13}$ [s^{-1}] $n_1 = 1.00$			$E_1 = 154.6$ [kJ/mol] $A_1 = 5.66 \times 10^9$ [s^{-1}] $n_1 = 0.86$			$E_1 = 114.0$ [kJ/mol] $A_1 = 2.45 \times 10^9$ [s^{-1}] $n_1 = 1.00$		
Stage 2	$E_2 = 220.3$ [(kJ/mol] $A_2 = 3.81 \times 10^{13}$ [s^{-1}] $n_2 = 0.69$			$E_2 = 188.4$ [kJ/mol] $A_2 = 3.15 \times 10^{10}$ [s^{-1}] $n_2 = 0. 69$			$E_2 = 220.4$ [(kJ/mol] $A_2 = 1.41 \times 10^{13}$ [s^{-1}] $n_2 = 0.61$			$E_2 = 154.4$ [kJ/mol] $A_2 = 2.50 \times 10^9$ [s^{-1}] $n_2 = 1.65$			$E_2 = 177.6$ [kJ/mol] $A_2 = 1.30 \times 10^{10}$ [s^{-1}] $n_2 = 0.69$		
h [K/min]	**5**	**7.5**	**10**	**5**	**7.5**	**10**	**5**	**7.5**	**10**	**5**	**7.5**	**10**	**5**	**10**	**15**
ν_1	0.18	0.19	0.20	0.12	0.17	0.19	0.09	0.13	0.13	0.58	0.58	0.58	0.17	0.17	0.17
ν_2	0.78	0.77	0.76	0.86	0.81	0.79	0.77	0.73	0.73	0.30	0.30	0.30	0.83	0.83	0.83
dev_{DTG} (%)	1.10	2.63	1.17	2.60	1.12	1.22	1.49	2.13	1.03	2.06	1.79	2.97	1.64	2.05	2.51
dev_{TG} (%)	0.46	0.70	0.45	0.50	0.24	0.57	0.35	0.60	0.17	0.72	1.52	0.33	0.86	0.88	0.62
ν_{1a}	0.19			0.16			0.12			0.58			0.17		
ν_{2a}	0.77			0.82			0.86			0.30			0.83		
dev_{DTG} (%)	1.24	2.63	1.25	2.83	1.24	1.91	1.44	2.04	1.05	2.06	1.79	2.97	1.64	2.05	2.51
dev_{TG} (%)	0.74	0.70	0.70	0.95	0.37	1.30	0.65	0.45	0.37	0.72	1.52	0.33	0.86	0.88	0.62

3.2. Kinetics of char oxidation

The formulation of a kinetic mechanism for the oxidation process is carried out using simultaneously the experimental curves at the three heating rates for each char sample. The estimated kinetic parameters and the deviations between the predicted and the measured curves are listed in Table 3. For comparison purposes, the data obtained from a re-evaluation of the oxidation curves of chars from washed fir wood [23] are also included. The component dynamics and the comparison between predictions and measurements for a heating rate of 5 K/min are shown in Fig. 8A–D while Fig. 9A–D report the comparison for the differential data at the various heating rates. The predicted dynamics of the two volatile fractions clearly reproduce the qualitative features already described in the analysis of the thermogravimetric curves. The first component corresponds to a devolatilization stage for the washed and the H_2SO_4 and $ZnCl_2$ treated samples with amounts of released volatiles corresponding to 18–20%, 12–19% and 9–13%, respectively. This is followed by the actual main oxidation step. In contrast, a large fraction of volatiles (58%) is released during the first reaction stage for the $Fe_2(SO_4)_3$ treated sample which can be considered as a low-temperature oxidation process ($n1 = 0.86$), also followed by a second oxidation stage.

The kinetic parameters take into account the qualitative and quantitative differences in the reactivity of the various char samples. As expected, the activation energies are affected by the characteristic temperatures and the shape of the differential curves. For the first

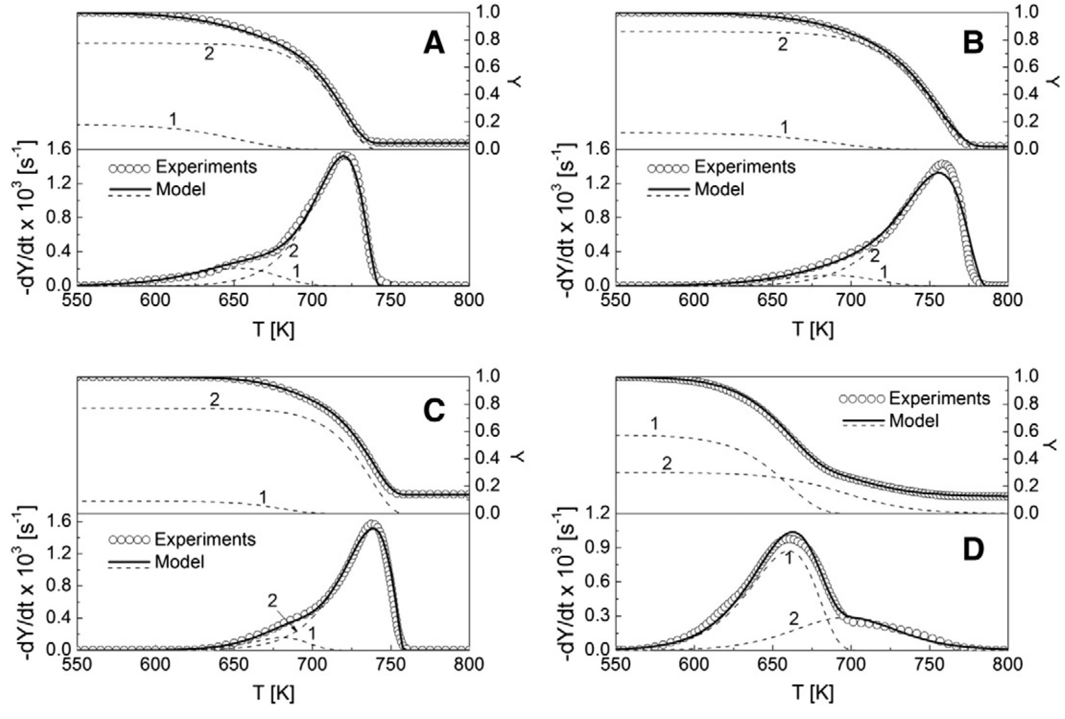

Fig. 8. A–D — Mass fraction and time derivative of the mass fraction versus temperature as measured (symbols) and predicted (solid lines) and predicted component dynamics (dashed lines) for chars produced from washed corncobs (A), H_2SO_4-treated corncobs (B), $ZnCl_2$-treated corncobs (C) and $Fe_2(SO_4)_3$-treated corncobs (D) (heating rate 5 K/min, kinetic parameters in Table 3).

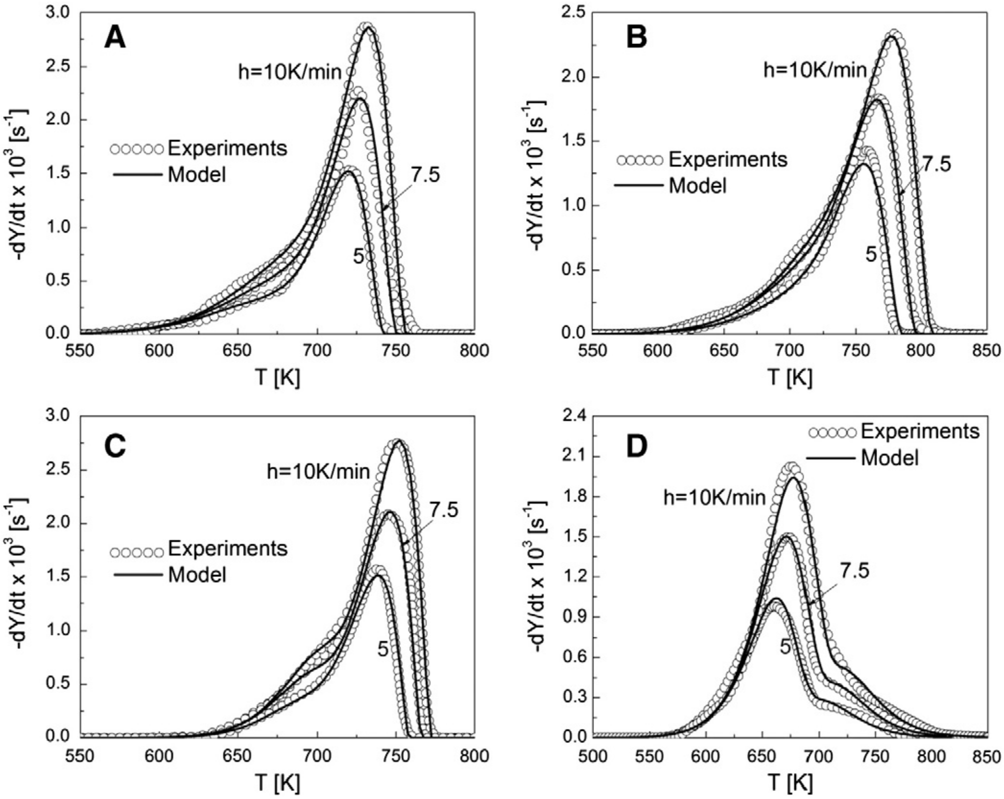

Fig. 9. A–D — Time derivative of the mass fraction versus temperature as measured (symbols) and predicted (solid lines) for chars produced from washed corncobs (A), H_2SO_4-treated corncobs (B), $ZnCl_2$-treated corncobs (C) and $Fe_2(SO_4)_3$-treated corncobs (D) (heating rates 5–10 K/min, kinetic parameters in Table 3).

(devolatilization) stage the activation energies are comparable for the washed samples and the H_2SO_4 treated sample (values in the range 114–132 kJ/mol) but a much higher value (210 kJ/mol) is estimated for the $ZnCl_2$ treated sample, essentially as a result of a more rapid initial increase in the devolatilization rate (a narrower ΔT_{p1}, Table 2). As for the second (oxidation) stage, in the first place, it can be observed that for the washed chars, a higher activation energy is estimated for corncobs with respect to fir wood (220 versus 178 kJ/mol), resulting from a process taking place over a narrower temperature range. On the other hand, the maximum and minimum activation energies are obtained for the $ZnCl_2$ and $Fe_2(SO_4)_3$ (220 and 154 kJ/mol) treated chars with an intermediate value for the H_2SO_4 treated sample. For the $Fe_2(SO_4)_3$ treated char a second slow oxidation step is required to describe the tailing zone of the differential curves.

It has been found that the estimated activation energies for the main oxidation peak are well correlated by the ratio of the parameter FWHM to the peak rate. The activation energies estimated for the chars under study and for other chars by this laboratory [15,23,24], with a re-evaluation for diammonium sulfate (DAS) treated samples ($A_1 = 1.92 \times 10^8 s^{-1}$, $E_1 = 144$ kJ/mol, $n_1 = 1$, $A_2 = 1.8 \times 10^7 s^{-1}$, $E_2 = 147$ kJ/mol, $n_2 = 0.73$), are reported in Fig. 10 on dependence of the ratio introduced above and evaluated for a heating rate of 5 K/min. It can be noticed that the lower the ratio value is the higher the activation energy. In other words, the estimated activation energy

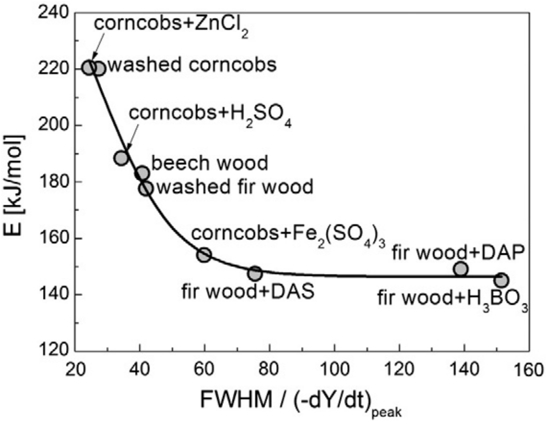

Fig. 10. Activation energy of the main combustion reaction, E, as a function of the ratio FWHM/ $(-dY/dt)_{peak}$ (evaluated for a heating rate of 5 K/min) for the chars from corncobs (this study) and washed fir wood, and fir wood treated with boric acid, diammonium sulfate (DAS) and diammonium phosphate (DAP) [15,23,24].

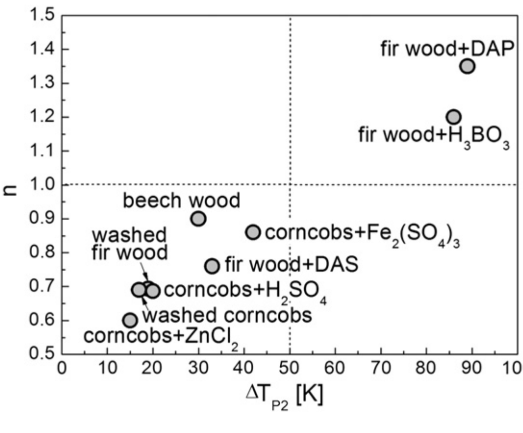

Fig. 11. Reaction order of the main combustion reaction, n, as a function of the temperature interval ΔT_{p2} (evaluated for a heating rate of 5 K/min) for the chars from corncobs (this study) and washed fir wood, and fir wood treated with boric acid, diammonium sulfate (DAS) and diammonium phosphate (DAP) [15,23,24].

for the oxidation reaction increases as the process tends to become faster (release of large quantities of volatiles, given high peak rate, over a narrow temperature interval). Then the pre-exponential factors are mainly determined by the position of the peak rate. Another important parameter is the exponent of the oxidation rate. It has been found that the actual estimated values are essentially dependent on how the rate, after the peak, decays to small values over the temperature interval ΔT_{p2}. Fig. 11 reports the estimated n values on dependence of ΔT_{p2} (evaluated at 5 K/min) for the chars examined in this study and others from previous studies of this laboratory [15,23,24]. It can be seen that the faster is the decay of the oxidation rate, the lower the estimated n. On an indicative basis, values of ΔT_{p2} below 50 K give rise to $n < 1$, as for all the chars examined in this study, whereas higher values are associated with $n > 1$, as for the chars produced by the pyrolysis of fir wood catalyzed by ammonium phosphate or boric acid.

The stoichiometric coefficients, ν_1 and ν_2, show small variations as the heating rate is increased due to the successively larger overlap between the activity of the two reactions of the kinetic mechanism. However, given that coupling reaction mechanisms with the description transport phenomena for the simulation of practical conversion systems usually requires constant coefficients, additional evaluations have also been made using average values (ν_{1a}, ν_{2a}). The results reported in Table 3 indicate that the deviations between predictions and measurements remain very small (and essentially coincident with the values found for variable coefficients) confirming the validity of the proposed kinetics.

4. Conclusions

Pyrolysis of corncobs catalyzed by some acidic substances (H_2SO_4, $Fe_2(SO_4)_3$ and $ZnCl_2$) has been shown to highly promote the production of furfural also increasing the yields of char which appears to be the product quantitatively more important. However, together with the yields of this product, catalysts added during pyrolysis also modify its behavior in combustion. It has been found that the reactivity of chars produced from acid-catalyzed pyrolysis is not significantly varied at low conversions but appears to be reduced at high conversions, especially in the case of the $Fe_2(SO_4)_3$ treatment.

The SEM and XRD analysis shows that chars produced from the H_2SO_4 catalyzed pyrolysis are those more similar to the product obtained from non-catalytic pyrolysis. However the attainment of the oxidation peak is retarded and significant rates are maintained over a wider temperature range. From the kinetic point of view, the process can be described with the usual two-step mechanism (devolatilization and oxidation) with an activation energy for the oxidation step which is lower than that obtained in the absence of catalysts (188 versus 220 kJ/mol). Chars produced by $ZnCl_2$ catalyzed pyrolysis are characterized by the presence of significant amounts of residues from the additive that appear to consist of ZnO which may also hinder to oxygen diffusion towards the active sites. Again, two main reaction zones are observed and the oxidation peak is significantly retarded but a large part of the conversion process is rather rapid resulting in a high activation energy (220 kJ/mol). On the whole, the activation energies for the oxidation reaction estimated for the chars obtained from the H_2SO_4 and $ZnCl_2$ catalyzed pyrolysis of corncobs (and for corncob pyrolysis) are in the range of values typically reported for biomass chars. Instead, the $Fe_2(SO_4)_3$ catalyzed pyrolysis gives rise to chars that are slowly oxidized already at low temperatures. Two oxidation reactions are required for an accurate description of the process with activation energies around 155 kJ/mol.

Acknowledgments

The authors thank Mr. Sabato Russo and Mr. Luciano Cortese (Istituto di Ricerche sulla Combustione, CNR, Napoli, Italy) for the SEM images and the XRD analysis of the char samples.

References

[1] C. Di Blasi, C. Branca, A. Galgano, Products and global weight loss rates of wood decomposition catalyzed by zinc chloride, Energy & Fuels 22 (2008) 663–670.

[2] A.S. Amarasekara, C.C. Ebede, Zinc chloride mediated degradation of cellulose at 200 °C and identification of products, Boresource Technology 100 (2009) 5301–5304.

[3] C. Branca, C. Di Blasi, A. Galgano, Pyrolysis of corncobs catalyzed by zinc chloride for furfural production, Industrial & Engineering Chemistry Research 49 (2010) 9743–9752.

[4] Q. Lu, C. Dong, X. Zhang, H. Tian, Y. Yang, X. Zhu, Selective fast pyrolysis of biomass impregnated with $ZnCl_2$ to produce furfural: analytical Py-GC/MS study, Journal of Analytical and Applied Pyrolysis 90 (2011) 204–212.

[5] C. Branca, A. Galgano, C. Blasi, M. Esposito, C. Di Blasi, H_2SO_4-catalyzed pyrolysis of corn cobs, Energy & Fuels 25 (2011) 359–369.

[6] C. Branca, C. Di Blasi, A. Galgano, Catalyst screening for the production of furfural from corncob pyrolysis, Energy & Fuels 26 (2012) 1520–1530.

[7] C. Di Blasi, C. Branca, A. Galgano, Biomass screening for the production of furfural via thermal decomposition, Industrial & Engineering Chemistry Research 49 (2010) 2658–2671.

[8] M.J. Antal, W.S.L. Mok, G. Varhegyi, T. Szekely, Review of methods for improving the yields of charcoal from biomass, Energy & Fuels 4 (1990) 221–225.

[9] M.J. Antal, E. Croiset, X. Dai, C. DeAlmeida, W.S. Mok, N. Norberg, J. Richard, M. Al Majthoub, High-yield biomass charcoal, Energy & Fuels 10 (1996) 652–658.

[10] A.M.C. Janse, H.G. de Jonge, W. Prins, W.P.M. van Swaaij, The combustion kinetics of char obtained by flash pyrolysis of pine wood, Industrial & Engineering Chemistry Research 37 (1998) 3909–3918.

[11] C. Di Blasi, F. Buonanno, C. Branca, Reactivities of some biomass chars in air, Carbon 37 (1999) 1227–1238.

[12] A. Marcilla, J.A. Conesa, M. Asensia, S.M. Garcia-Garcia, Thermal treatment and foaming of chars obtained from almond shells: kinetic study, Fuel 79 (2000) 829–836.

[13] A. Zolin, A. Jensen, P.A. Jensen, F. Frandsen, K. Dam-Johansen, The influence of inorganic materials on the thermal deactivation of fuel chars, Energy and Fuels 15 (2001) 1110–1122.

[14] J. Adanez, L.F. de Diego, F. Garcia-Labiano, A. Abad, J.C. Abadanes, Determination of biomass char combustion reactivities for FBC applications by a combined method, Industrial & Engineering Chemistry Research 40 (2001) 4317–4323.

[15] C. Branca, C. Di Blasi, Devolatilization and combustion kinetics of wood chars, Energy & Fuels 17 (2003) 1609–1615.

[16] M. Guerrero, M.P. Ruiz, M.U. Alzueta, R. Bilbao, A. Millera, Pyrolysis of eucalyptus at different heating rates: studies of char characterization on oxidative reactivity, Journal of Analytical and Applied Pyrolysis 74 (2005) 307–314.

[17] M. Guerrero, M.P. Ruiz, A. Millera, M.U. Alzueta, R. Bilbao, Characterization of biomass chars formed under different devolatilization conditions: differences between rice husks and eucalyptus, Energy & Fuels 22 (2008) (2008) 1275–1284.

[18] M. Guerrero, M.P. Ruiz, A. Millera, M.U. Alzueta, R. Bilbao, Oxidation kinetics of eucalyptus chars produced at low and high heating rates, Energy & Fuels 22 (2008) 2084–2090.

[19] G. Varhegyi, E. Meszaros, M.J. Antal, J. Bourke, E. Jakab, Combustion kinetics of corncob charcoal and partially demineralized corncob charcoal in the kinetic regime, Industrial & Engineering Chemistry Research 45 (2006) 4962–4970.

[20] C. Branca, C. Di Blasi, Combustion kinetics of secondary biomass chars in the kinetic regime, Energy & Fuels 24 (2010) 5741–5750.

[21] A. Anca-Couce, N. Zobel, A. Berger, F. Behrendt, Smouldering of pine wood, Combustion and Flame 159 (2012) 1798-1719.

[22] Y. Sekiguchi, F. Shafizadeh, The effect of inorganic additives on the formation, composition and combustion of cellulosic char, Journal of Applied Polymer Science 29 (1984) 1267–1286.

[23] C. Branca, C. Di Blasi, Oxidation characteristics of chars generated from wood impregnated with $(NH_4)_2HPO_4$ and $(NH_4)_2SO_4$, Thermochimica Acta 456 (2007) 120–127.

[24] C. Di Blasi, C. Branca, A. Galgano, Flame retarding of wood by impregnation with boric acid — Pyrolysis products and char oxidation rates, Polymer Degradation and Stability 92 (2007) (2007) 752–764.

[25] G.R. Ponder, G.N. Richards, Oxygen and CO_2 gasification of chars from wood treated with iron (II) and iron (III) sulfates, Energy & Fuels 8 (1994) 705–713.

[26] C. Di Blasi, Combustion and gasification rates of lignocellulosic chars, Progress in Energy and Combustion Science 35 (2009) 121–140.

[27] C. Branca, C. Di Blasi, Global intrinsic kinetics of wood oxidation, Fuel 83 (2004) 81–87.

[28] C. Branca, A. Iannace, C. Di Blasi, Devolatilization and combustion kinetics of Quercus Cerris bark, Energy & Fuels 21 (2007) 1078–1084.

[29] C. Branca, C. Di Blasi, Oxidative devolatilization kinetics of wood impregnated with two ammonium salts, Fire Safety Journal 43 (2008) 317–324.

[30] C. Branca, C. Di Blasi, Semi-global mechanisms for the oxidation of diammonium phosphate impregnated wood, Journal of Analytical and Applied Pyrolysis 91 (2011) 97–104.

[31] M. Brostrom, A. Nordin, L. Pommer, C. Branca, C. Di Blasi, Influence of torrefaction on the devolatilization and oxidation kinetics of wood, Journal of Analytical and Applied Pyrolysis 96 (2012) 100–109.

[32] C. Branca, C. Di Blasi, A unified mechanism of the combustion reactions of lignocellulosic fuels, Thermochimica Acta 565 (2013) 58–64.

[33] C. Branca, C. Di Blasi, H. Horacek, Analysis of the combustion kinetics and the thermal behavior of an intumescent system, Industrial & Engineering Chemistry Research 41 (2002) 2104–2114.

[34] C. Branca, A. Albano, C. Di Blasi, Critical evaluation of wood devolatilization mechanisms, Thermochimica Acta 429 (2005) 133–141.

[35] J.A. Conesa, A. Marcilla, J.A. Caballero, R. Font, Comments on the validity and utility of the different methods for kinetic analysis of thermogravimetric data, Journal of Analytical and Applied Pyrolysis 58–59 (2001) 617–633.

[36] J.A. Caballero, J.A. Conesa, Mathematical considerations for nonisothermal kinetics in thermal decomposition, Journal of Analytical and Applied Pyrolysis 73 (2005) 85–100.

[37] G. Varhegyi, M.G. Gronli, C. Di Blasi, Effects of sample origin, extraction and hot water washing on the devolatilization kinetics of chestnut wood, Industrial & Engineering Chemistry Research 43 (2004) 2356–2367.

[38] J. Hayashi, A. Kazehaya, K. Muroyama, A.P. Watkinson, Preparation of activated carbon from lignin by chemical activation, Carbon 38 (2000) 1873–1878.

[39] F. Shafizadeh, A.G.W. Bradbury, W.F. De Groot, T.W. Aanerud, Role of inorganic additives in the smoldering combustion of cotton cellulose, Industrial & Engineering Chemistry Product Research and Development 21 (1982) 97–101.

[40] M.S.R. Swamy, T.P. Prasad, B.R. Sant, Thermal analysis of ferrous sulfate pentahydrate in air, Journal Thermal Analysis 15 (1979) 307–314.

[41] A.G.W. Bradbury, F. Shafizadeh, Role of oxygen chemisorption in low-temperature ignition of cellulose, Combustion and Flame 37 (1980) 85–89.

[42] A.G.W. Bradbury, F. Shafizadeh, Chemisorption of oxygen on cellulose char, Carbon 18 (1980) 109–116.

[43] F. Shafizadeh, Y. Sekiguchi, Oxidation of chars during smoldering combustion of cellulosic materials, Combustion and Flame 55 (1984) 171–179.

[44] M. Jagtoyen, F. Derbyshire, Activated carbons from yellow poplar and white oak by H_3PO_4 activation, Carbon 36 (1998) 1085–1097.